Adiabatic Effectiveness Measurements and Predictions of Leakage Flows Along a Blade Endwall

W. W. Ranson

K. A. Thole

Department of Mechanical Engineering,
Virginia Polytechnic Institute and State University,
Blacksburg, VA 24060

F. J. Cunha

Pratt & Whitney,
United Technologies Corporation,
East Hartford, CT 06108

Traditional cooling schemes have been developed to cool turbine blades using high-pressure compressor air that bypasses the combustor. This high-pressure forces cooling air into the hot main gas path through seal slots. While parasitic leakages can provide a cooling benefit, they also represent aerodynamic losses. The results from the combined experimental and computational studies reported in this paper address the cooling benefit from leakage flows that occur along the platform of a first stage turbine blade. A scaled-up, blade geometry with an upstream slot, a mid-passage slot, and a downstream slot was tested in a linear cascade placed in a low-speed wind tunnel. Results show that the leakage flow through the mid-passage gap provides only a small cooling benefit to the platform. There is little to no benefit to the blade platform that results by increasing the coolant flow through the mid-passage gap. Unlike the mid-passage gap, leakage flow from the upstream slot provides good cooling to the platform surface, particularly in certain regions of the platform. Relatively good agreement was observed between the computational and experimental results, although computations overpredicted the cooling. [DOI: 10.1115/1.1929809]

Introduction

First stage turbine blades are exposed to harsh operating conditions and temperatures that exceed the melting temperature of the blades. In nearly all gas turbine engines, cooler air from the compressor bypasses the combustion chamber. Traditional techniques have been used to cool turbine blades such as impingement cooling, film cooling, and convective cooling. Unfortunately, sealing interfaces inherent to rotating machinery results in gaps for high-pressure cooling flow to leak into the main hot gas path. Gaps exist between vanes and blades and between adjacent blades.

The elimination of leakage flows provides better performance. However, leakage flows also provide some cooling. Therefore, it is important to understand the effect of leakage flows on the cooling of turbine blade platforms. The work presented in this paper quantifies the benefit of coolant leakage in the platform region of a turbine blade in a linear cascade.

A detailed experimental and computational study of a turbine blade with leakage flows from a backward facing upstream slot, which represents the gap between vane and blade stages, a featherseal gap, which represents the mid-passage gap between adjacent airfoils, and a downstream slot, which represents the gap between the next turbine stage. In particular, the focus was on the effects of different leakage flow rates on the adiabatic effectiveness levels along the blade platform. Computational results were compared to experimental measurements. Additionally, thermal field measurements were taken.

Past Studies

Numerous papers have benchmarked the secondary flow fields and their effects on heat transfer along an uncooled endwall in linear cascades (Langston et al. [1], Graziani et al. [2], Sharma and Butler [3], Goldstein and Spores [4], and Kang et al. [5]). Most of the geometries that were used, however, were representative of vane designs, which typically have much different characteristics than a blade design. Though these studies have yielded a fundamental understanding of the complex flows along a vane endwall, they have not directly addressed the effects of leakage flows.

Some of the earliest work related to endwall cooling by leakage flows was performed by Blair [6], who used a two-dimensional flush slot upstream of a vane geometry. Increases in cooling effectiveness along the endwall were observed as the flow through the slot was increased. In a similar study of coolant upstream of a vane passage, Burd et al. [7] studied the effects of an upstream flush, 45° slot. By using coolant flows as high as 6% of the total passage flow, good cooling was observed over the endwall and both sides of the vanes. A study by Colban and Thole [8] measured the effects of changing the combustor liner film-cooling and junction slot flows on the effectiveness levels along the endwall of a first stage turbine vane. Their results show the coolant from the slot was not uniform across the exit, with coolant accumulating along the endwall near the suction side of the vane. Coolant injection from the upstream combustor liner causes different total pressure profiles entering the vane passage that in turn changed the secondary flow field. Studies by Zhang and Jaiswal [9], Nicklas [10], and Knost and Thole [11] have studied the combined effects of upstream slot cooling and film hole cooling in a turbine vane passage. Results showed that slots upstream of the passage provided nonuniform cooling along the vane endwall with a difficult region to cool being the pressure side.

Using a simple flat plate geometry with no turbine airfoils, Yu and Chyu [12] studied the influence of gap leakage downstream of injection cooling holes. They observed that for a moderate level of film cooling upstream of a coolant slot, the combined presence of the gap promoted better coolant film protection. However, as the film-cooling flow was increased, the coolant from the gap appeared to lift the slot flow coolant from the wall, resulting in decreased adiabatic effectiveness.

The only known study of flows from a featherseal-like slot within an airfoil passage was performed by Aunapu et al. [13].

Contributed by the Turbomachinery Division of THE AMERICAN SOCIETY OF MECHANICAL ENGINEERS for publication in the JOURNAL OF TURBOMACHINERY. Manuscript received by the ASME Turbomachinery Division September 26, 2004; final revision received January 18, 2005. Editor: D. Wisler.

Table 1 Blade geometry

Blade parameter	Value
Scaling factor	11X
Inlet angle	19.2°
Blade angle	20°
Inlet Reynolds number on true chord	3.0*E*+05
True Chord/Axial chord	1.05
Pitch/Axial chord	0.79
Span/Axial chord	1.28

They used blowing through a passage gap in an attempt to reduce the effects of a passage vortex. They hypothesized endwall blowing in the blade passage would have a similar affect seen by Chung and Simon [14], who used a fence in the middle of the passage to lift the passage vortex. Aunapu et al. [13] observed that endwall jets in the center of the blade passage effectively altered the path of the pressure side leg of the vortex. Unfortunately, the increased blowing caused higher turbulence and higher aerodynamic losses.

In summary, there have been no studies directly addressing the benefits of coolant leakage flows from small gaps within adjacent airfoil passages. Moreover, there have been no studies with combined upstream and mid-passage coolant leakage through the platform of a turbine blade. It is important to understand the effect of coolant flow from leakage points in the hub region to further the technology of turbine blade cooling.

Experimental Procedures

The blade geometry used for this work represents a modified design for the first stage of a gas turbine. The modifications from the original engine geometry were made to ensure correctly scaled pressure loading around the blades when operating in a low-speed testing environment. To ensure good measurement resolution while matching realistic engine flows, the blades were scaled up 11×. The turbine blade geometry is two dimensional, having no variation in the span direction. This uniform cross section represents the cross section at the blade–hub intersection. Additionally, the platform was modeled as a flat surface with no curvature. A summary of geometry and flow conditions is given in Table 1.

The three main leakage features studied were the upstream slot, the featherseal, and the aft slot, as shown in Fig. 1. Even though in actual gas turbines the sizes of these gaps change with temperature, the sizes of the leakage features were held constant for this study. While the aft gap was a slot with a width of 5.5% of the blade chord, the upstream slot was a backward facing slot at an angle of 17 deg. Figure 2 shows a side view of the upstream slot that was a backward facing step, and the fillet that was used at the base of the blades. The locations where the featherseal attaches to the front and aft slots are referred to as the front and aft gutter, respectively. The lengths and widths of the leakage features are summarized in Table 2.

The features were fed by three independently controlled plenums, including one for the featherseal, a second for the upstream slot and front gutter, and a third for the aft slot and aft gutter. Thus, the leakage settings for the front slot controlled the flow out of both the front slot and front gutter, and the leakage settings for the aft slot controlled flow out of both the aft slot and the aft gutter.

The test section used for this study was a four blade, three passage, linear cascade where the flow angles were matched by staggering the blades. To compare the effects of the featherseal on cooling of the endwall, the middle passage did not contain a featherseal. Figure 3 shows a top view of the test rig. By setting the flows from the upstream normal jets, the inlet turbulence intensity was 10% and the length scale was 11 cm. Inlet velocity was 11 m/s. To ensure adiabatic measurements, the platform region was constructed out of low thermal conductivity foam

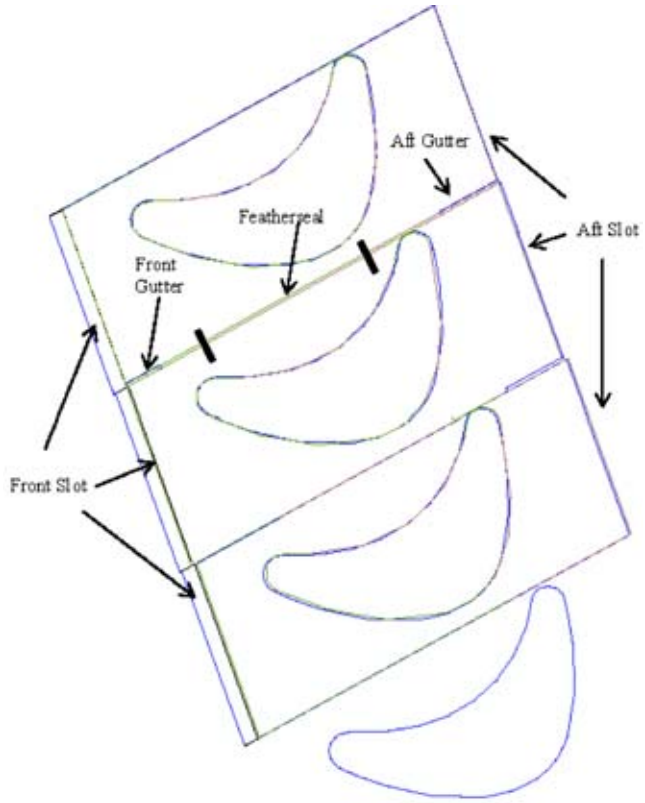

Fig. 1 Schematic of test section (thermal rake locations for Figs. 10 and 11 indicated)

(0.021 W/m K). The blades were also constructed with low thermal conductivity foam and coated with a black Teflon® film. Pressure taps were installed in the midspan of the blades to verify

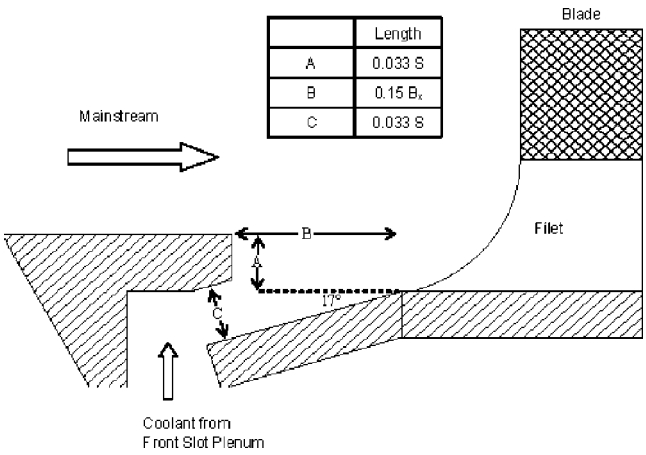

Fig. 2 Side view of backward facing step in the front slot, which contains the front gutter

Table 2 Sizes of scaled test leakage features

	Axial length	Gap width
Front slot	2.7 *P*	0.048 B_x
Aft slot	2.7 *P*	0.055 B_x
Feather seal	1.3 B_x	0.0013 *P*
Front gutter	0.14 B_x	0.008 *P*
Aft gutter	0.26 B_x	0.008 *P*

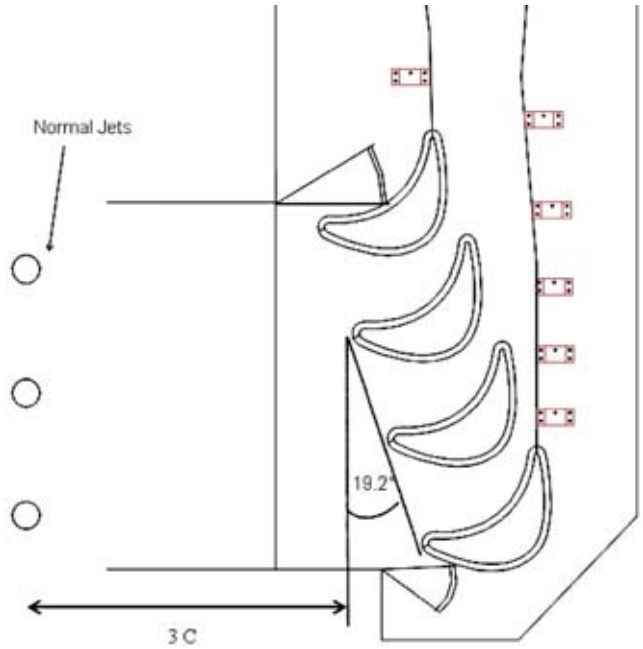

Fig. 3 Schematic of linear blade cascade, including flexible walls and upstream normal jets

the correct pressure distribution around the blades. By adjusting the flexible walls shown in Fig. 3, periodicity between the passages was ensured. Good agreement was indicated between the nondimensional pressure distribution at the midspan obtained from computational predictions and experimental measurements shown in Fig. 4.

A set of simulations focused on investigating the effects of leakage flows from the various slots, as shown in Table 3. All of the flows are listed as a percent of the total inlet core flow. The aft slot flow was set at a constant 1.5% of the inlet flow as the aft slot is sufficiently downstream of the platform region of the blades in this study. In actual turbine engines, the aft slot of this study is the front slot of the next set of stator blades.

Since the front and aft slots were supplied by flow from the bottom passage of the wind tunnel, the mass flow through the slots was calculated from the pressure difference measured between pressure taps in the plenums and the platform surface. To calculate

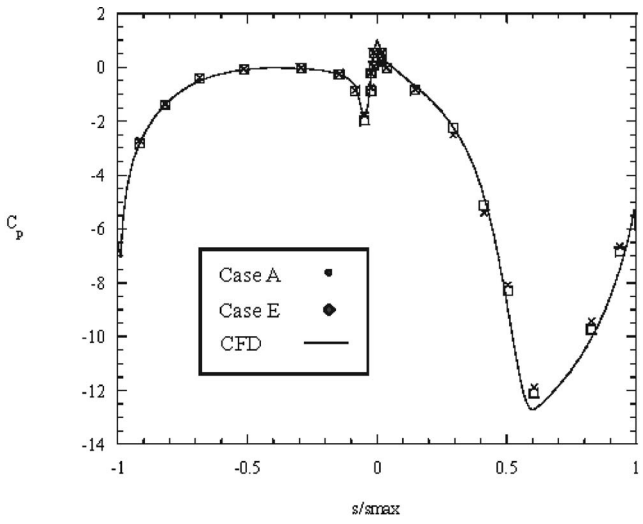

Fig. 4 Measured and predicted pressure distributions

Table 3 Text matrix. *denotes CFD modeling.

	Percent of total inlet mass flow				
	Case A*	Case B*	Case C*	Case D*	Case E
Featherseal	0.25%	0.50%	0.75%	0.75%	0.50%
Front slot	1.50%	1.50%	1.50%	2.00%	0.50%
Aft slot	1.50%	1.50%	1.50%	1.50%	1.50%
Total	3.25%	3.50%	3.75%	4.25%	2.50%

the actual mass flow from this ideal calculation, a discharge coefficient of 0.6 was assumed. The featherseal plenum was fed by compressed air, thus the mass flow was measured directly with a laminar flow element (LFE).

To accurately measure the adiabatic effectiveness levels along the endwall, we used infrared thermography. Since the viewing area of the infrared camera is dictated by the distance between the camera and the platform region (which is the blade span), 19 viewing ports were constructed in the top surface of the test rig to capture the entire platform region. To reduce the precision uncertainty in the infrared images, 5 images were taken at each of the 19 view ports for every test case. Each of the five images was averaged into one image, which was then calibrated based upon thermocouple measurements placed in the endwall. Using an in-house MATLAB [15] code, each of the 19 images was oriented in their correct position to create a complete temperature map of the entire platform region. The resulting temperature is reported in terms of adiabatic effectiveness, η. For all the testing, the typical difference between coolant and mainstream temperature was approximately 25°C. In addition to infrared thermography, thermal field measurements were taken perpendicular the featherseal at two locations, 9% and 27% of the chord length from the front slot. The thermal fields were measured using a rake consisting of 21 thermocouples that were evenly spaced 5.1 mm apart.

For the static pressure measurements, the total uncertainty in C_p was calculated to be 7.5%. The C_p uncertainty was high because this pressure quantity is calculated from three separate pressure measurements, each of which had an uncertainty that propagates through the calculation. For the temperature measurements, all of the thermocouples were calibrated in an ice bath to have a bias uncertainty of 0.2°C. The combined temperature and pressure uncertainties resulted in a mass flow uncertainty of 0.0046 kg/s, which was 11.5% of the low flow conditions and 7.6% of the high flow conditions. This uncertainty in the temperature measurement yields an uncertainty in the thermal field measurements (Θ) of 0.03. The uncertainty in the adiabatic effectiveness (η) measurements, which includes the uncertainty of the infrared camera, was 0.035, which is 17.5% of η=0.2 and 4.4% of η=0.8. The turbulence level uncertainty was 1.8%.

Computational Methodology

A commercially available computational fluid dynamics (CFD) code, FLUENT [16], was used to perform all the simulations. FLUENT is a pressure-based, incompressible flow solver that can be used with structured or unstructured grids. An unstructured grid was used for the study presented in this paper. Solutions were obtained by numerically solving the Navier–Stokes and energy equation through a control volume technique. All geometric construction and meshing were performed with GAMBIT.

Computations were performed on a single turbine blade exposed to periodic conditions along all boundaries in the pitchwise direction. Inlet conditions to the model were set as a uniform inlet velocity at one chord length upstream of the blade. Because the inlet flow from the front rim was at most 2.0% (Table 3) of the passage flow, the inlet passage flow was maintained the same for all the simulations. Flow angles were set to match those conditions of the experiments as well as the scaled values for the engine

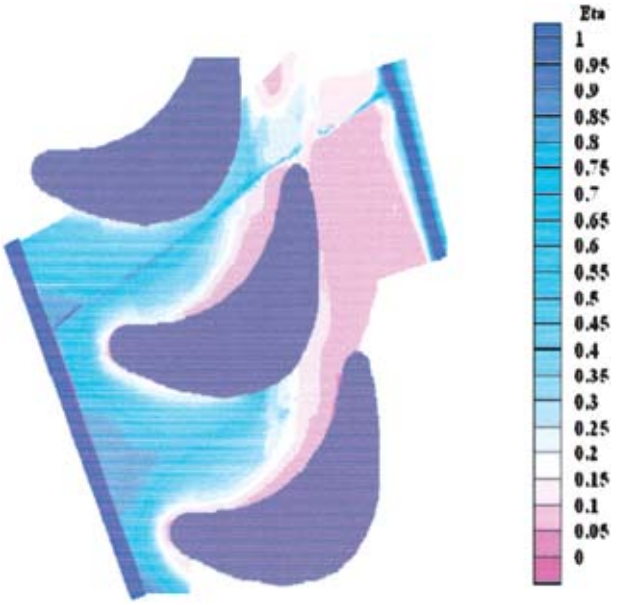

Fig. 5 Adiabatic effectiveness measurements for 1.5% front slot and aft slot, and 0.25% featherseal flow

while turbulence levels were set to 10%. Three separate inflow boundary conditions were used to supply each of the leakage features. The density ratio of the coolant to the mainstream was nearly one ($\sim$1.06) for all of the experimental and computational cases. An outflow boundary was applied 1.5 chords downstream of the blade.

Only one-half of the blade span was modeled. Comparisons made between the entire span and half the span showed no differences in the resulting pressure or thermal results. Thus, only half the span was simulated extending from the platform to the midspan. The boundary conditions at the midspan were set as a slip wall (frictionless) while a no-slip boundary condition was applied at the platform. Although the relative motion of rotor blades to stator vanes can be computationally modeled, that boundary condition was not examined in order to match the experimental studies in a linear blade cascade.

All computations were performed using the RNG κ-ε turbulence model with nonequilibrium wall functions whereby the near-wall region was resolved to y^+ values ranging between 30 and 60. Mesh insensitivity was confirmed though several grid adaptions based upon viscous wall values, velocity gradients, and temperature gradients. Typical mesh sizes were composed of 1.4 million cells. Adaptions from a mesh of 1.3 million to 2.0 million resulted in variations of the pitchwise-averaged adiabatic effectiveness values of $\Delta\eta = \pm 0.008$ at a level of $\eta = 0.4$. The convergence of residuals for continuity, x-momentum, y-momentum, z-momentum, κ and ε were resolved to levels of 10^{-4}. The energy equation was set to a convergence of residuals of 10^{-7}. Typical convergence required 1500 iterations for convergence to be met.

Experimental Results

As was indicated in the test matrix, Table 3, the data for the first three cases (Cases A–C) were simulated to determine the effect of flow through the featherseal only while flows through all of the other slots remained the same. The last three cases in Table 3 (Cases C–E) show the effects of changing the coolant flow levels through the upstream backward-facing slot.

Featherseal Coolant Effects. Figure 5 shows adiabatic effectiveness measurements for the featherseal flow of 0.25% of the total passage flow and the front and aft slot each having 1.5% of the total passage (Case A). Recall that only one of the passages actually contains the featherseal (top passage in Fig. 5). The size of the blade images in Fig. 5 is slightly larger the blade geometry since these images include the fillet at the blade–endwall juncture. As shown in Fig. 5, the front slot leakage dominates the cooling of the platform region with adiabatic effectiveness measurements between 0.8 and 0.9 just downstream of the front slot. Although the coolant from the front slot provides ample cooling of the endwall region downstream of the slot, the leading edges of the blades are not cooled. An examination of the lower passage in Fig. 5 shows the front slot coolant has almost no effect on cooling the pressure side of the blades, as the adiabatic effectiveness values near the trailing edge pressure side of the blades are close to zero. The lack of pressure side cooling from the front slot matches the results of Colban et al. [8], who also showed that even with large coolant flows from their backward-facing slot, cooling was not present near the pressure side of the vane. Additionally shown in Fig. 5, toward the trailing edge of the blades, the upstream slot flow has no affect on the aft portion of the blade along the suction side. As shown in the bottom passage, the coolant from the upstream slot affects only the first 60% of the chord length. In contrast to the lower passage, the coolant leakage from the featherseal in the upper passage provides some cooling along the aft portion of the blade along the suction side. Without the featherseal, the adiabatic effectiveness values near the trailing edge of the suction side are below 0.2, while the adiabatic effectiveness values near the trailing edge with the featherseal coolant are near 0.6. The flow from the featherseal, however, does not have a beneficial effect on the pressure side.

Coolant from the featherseal has more of an effect on the suction side of the blade because the inherent pressure distribution between the blades tends to pull flow from the pressure side to the suction side of the blades. Although flow is swept toward the suction side of the blades near the trailing edge of the blade passage, coolant from the featherseal at the passage inlet is swept toward the pressure side of the blades. In addition to the effects of pressure side to suction side flow, the featherseal coolant is also affected by the passage vortex. An analysis of this phenomenon is discussed in the Thermal Field Measurement section of this paper.

The flow is initially swept toward the pressure side of the blades because of the angle that the mainstream flow enters the test passage. The mainstream flow initially causes the featherseal coolant to flow toward the pressure side as the momentum of the flow pushes the coolant towards the pressure side of the blades. However, as the pressure distribution along the blade endwall overcomes the inlet flow momentum, the coolant from the featherseal is then swept toward the suction side of the blades. This effect will be further illustrated through the CFD results. In Fig. 5, at the inlet to the passage, the coolant is visible with an adiabatic effectiveness level of nearly one (indicating the coolant temperature). Toward the trailing edge of the featherseal, the coolant flow is less visible. The decrease in observable featherseal coolant is due to the direction of the mainstream flow.

Toward the beginning of the blade passage, the mainstream flow is nearly parallel to the featherseal. However, toward the trailing edge, the flow is nearly perpendicular to the featherseal, which sweeps flow away from the featherseal. Though there are less visible adiabatic effectiveness levels near the trailing edge, the cooling benefits of the featherseal are more observable near the trailing edge of the blades, where the effectiveness levels increase from 0.1 to 0.3. Figure 5 also shows the aft slot has less effect on the cooling near the blades than either the front slot or featherseal, as expected.

To determine the effects of the featherseal, we tested featherseal coolant levels of 0.25%, 0.5%, and 0.75% of the total passage flow while maintaining the front and aft slots each at 1.5% (Cases A–C). Figures 6(a)–6(c) show the measurements for the 0.25%, 0.5%, and 0.75% featherseal flow while the coolant levels for the front and aft slot were maintained the same at 1.5% each. All three cases show the same trends and same adiabatic effectiveness val-

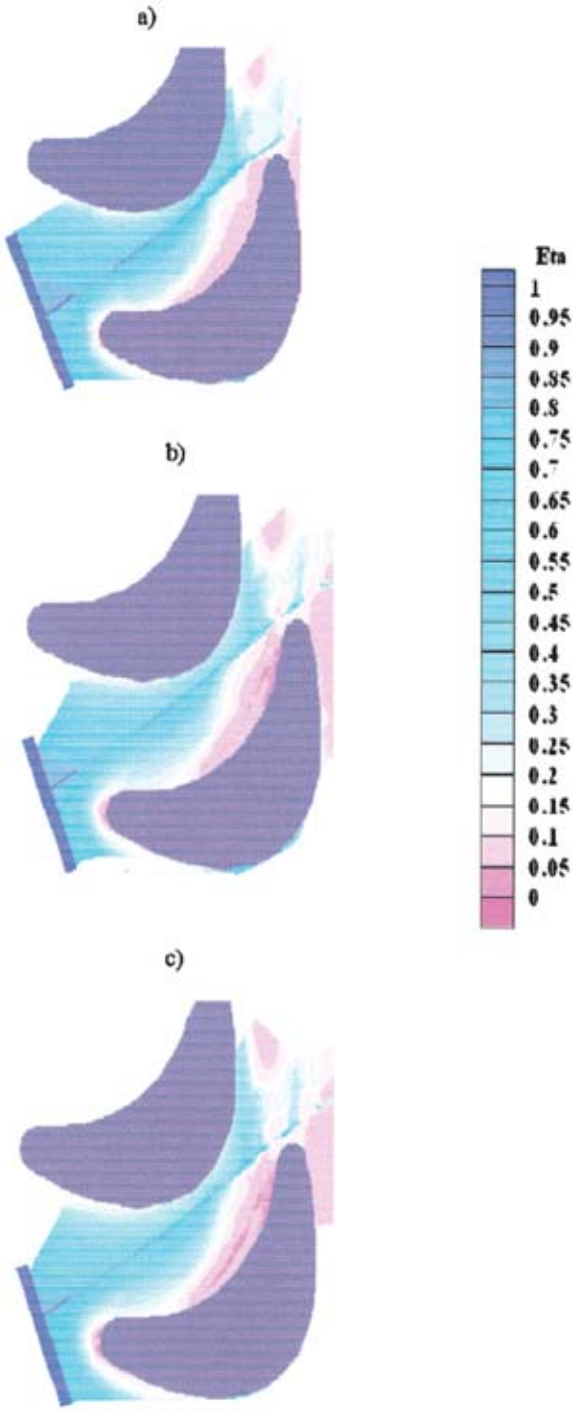

Fig. 6 Adiabatic effectiveness measurements for 1.5% front and aft slot flow with (*a*) 0.25%, (*b*) 0.5%, and (*c*) 0.75% featherseal flow

ues around the featherseal. The results in Figs. 6(*a*)–6(*c*) indicate that as the flow out of the featherseal is increased, the momentum of the coolant flow out of the featherseal causes the coolant to be blown into the mainstream, providing little cooling benefit. Since the coolant flow is swept away from the platform quickly, even at low flow conditions, it is not surprising that increasing the featherseal flow does not increase the platform cooling.

To quantify the lack of additional cooling from increasing the featherseal flow, laterally averaged adiabatic effectiveness values were calculated for the first three cases shown. Laterally averaged values were calculated based upon averages of all the adiabatic

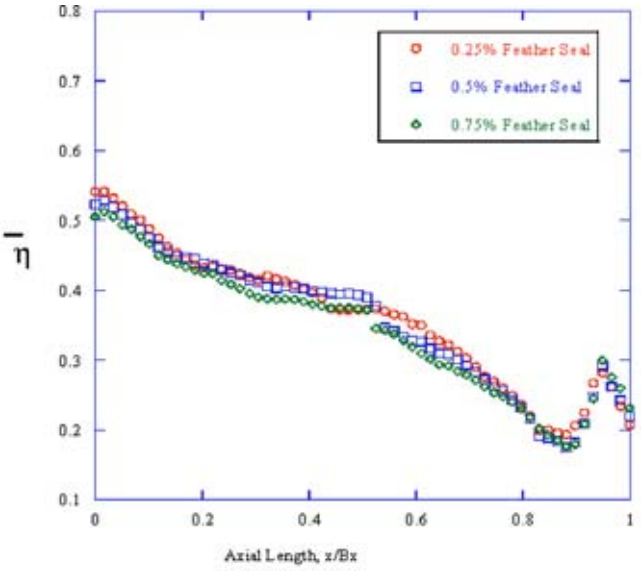

Fig. 7 Average adiabatic effectiveness measurements for the data shown in Figs. 6(*a*)–6(*c*)

effectiveness values along a line perpendicular to the featherseal. Figure 7 shows the averaged adiabatic effectiveness measurements for Figs. 6(*a*)–6(*c*). The results shown in Fig. 7 indicate that there is no cooling increase with increased featherseal flows. The increase in the laterally averaged adiabatic effectiveness values near $x/B_x=0.9$ is caused by the featherseal effects on the trailing edge suction side of the blades. Though it appears the higher featherseal flow case provides the least cooling, the uncertainty of the measurements prevents any definite conclusions from being made. There is no effect with increasing featherseal flow.

For each of the three cases shown in Figs. 6(*a*)–6(*c*), more flow exits from the trailing edge of the featherseal because the static-pressure is lower, in comparison with the leading edge. A calculation of the momentum flux (as shown in later sections) indicates that the momentum flux ratio of the slot flow to the mainstream is nearly constant across the featherseal. As will be shown through the CFD results, the coolant exiting the leading edge of the featherseal is directed by the mainstream flow toward the pressure side of the blade. The coolant exiting the trailing edge of the feather seal is directed toward the suction side of the blade. The effects from the front slot dominate the cooling of the leading edge region blade platform. Because of the dominating effect of the upstream slot and because more coolant exits the trailing edge, the largest cooling benefit from the featherseal slot is near the trailing edge. Though the featherseal does provide some platform cooling, increases in the coolant flow do not increase this cooling.

Upstream Slot Coolant Effects. Although increasing the featherseal flow does not increase the cooling on the endwall, increasing the coolant from the front slot increases the endwall cooling. Figures 8(*a*)–8(*c*) show adiabatic effectiveness measurements when the front slot flow is increased from 0.5% to 1.5% to 2.0% while the featherseal remains at 0.25% and the aft slot also remains the same at 1.5%. As the front slot cooling is increased from 1.5% to 2.0%, the temperature on the pressure side of the blades is reduced. Additionally, coolant was observed wrapping around the suction side of the blades from the passage without the featherseal. The higher front rim flow is able to cool farther into the passage. With the low front slot cooling, the temperature measurements on the trailing edges of both the pressure side and suction side of the blades is nearly the mainstream temperature, as no coolant is present.

Laterally averaged adiabatic effectiveness measurements, shown in Fig. 9, support the results of increased endwall cooling

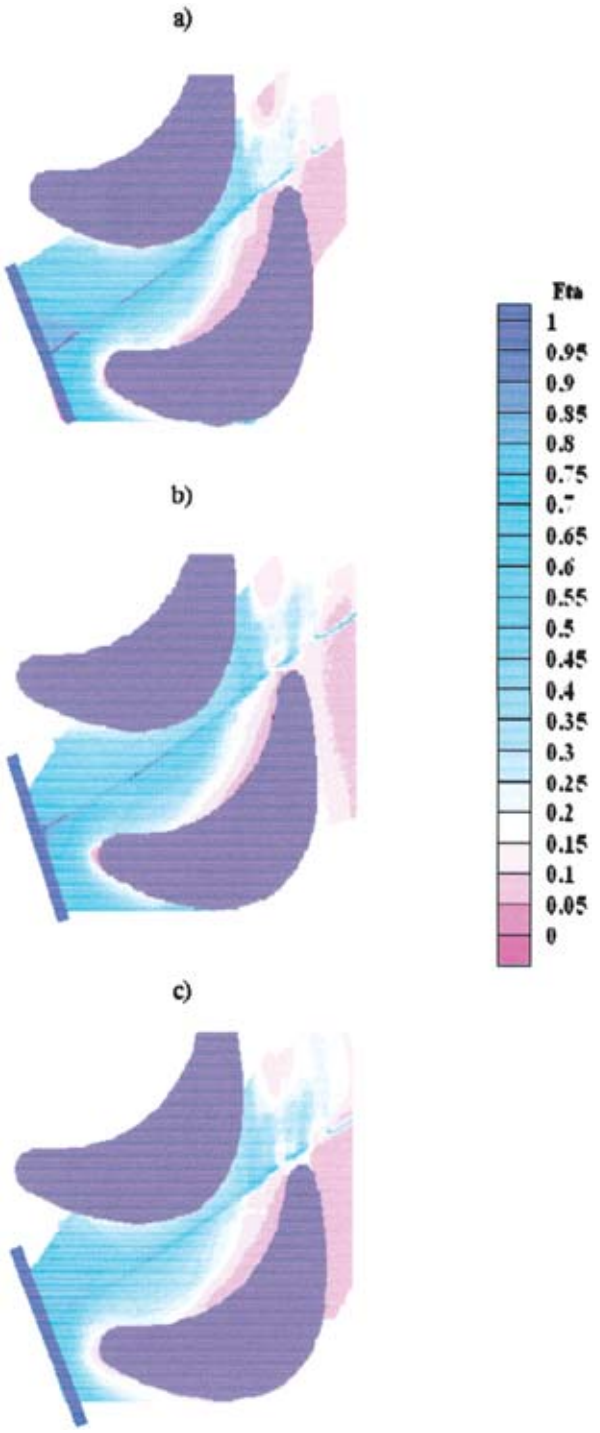

Fig. 8 Adiabatic effectiveness measurements for 0.25% featherseal flow and 1.5% aft slot flow with (*a*) 1.5% front slot, (*b*) 2.0% front slot, and (*c*) 0.5% front slot flow

with increased front slot flow. Throughout the entire blade passage, the average adiabatic effectiveness values are highest for the front slot leakage flow of 2.0%, and lowest for the front slot leakage of 0.5%. Interestingly, there was not a substantial decrease in average cooling with the 0.5% case, as the featherseal flow is able to provide cooling, especially near the trailing edge suction side of the blades. Though the local differences in Fig. 9 appear larger than those first observed in Fig. 8, it is important to note that Fig. 9 is an average across the whole passage, which includes the large temperature variations near the blade walls.

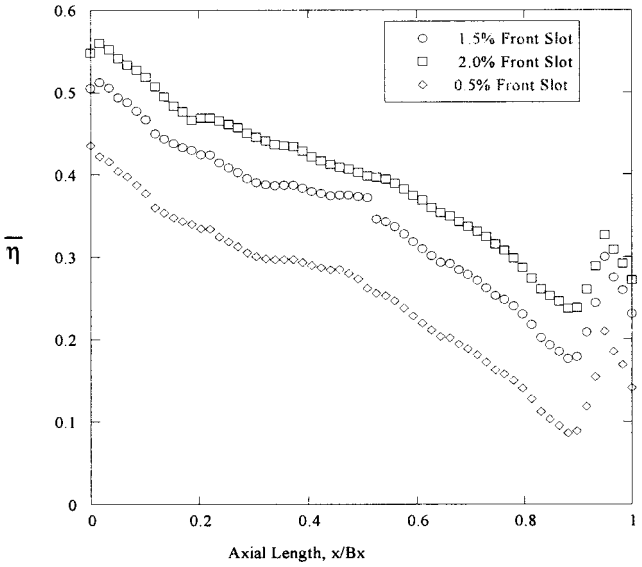

Fig. 9 Average adiabatic effectiveness measurements for the data shown in Figs. 8(*a*)–8(*c*)

Thermal Field Measurements

To better understand the leakage effects, thermal field measurements at two locations along the platform were taken that include the following: near the leading edge of the featherseal and near the trailing edge of the featherseal, as shown by the lines in Fig. 1. For these measurements the upstream slot was set at 1.5% coolant flow and the featherseal flow was varied from 0.25% to 0.75%. The thermal field measurements near the leading edge of the featherseal for the low flow condition are shown in Fig. 10(*a*), and for the high flow in Fig. 10(*b*).

These figures are shown looking downstream from the passage inlet (the pressure side of the blades is on the right-hand side of the contour plot). The location of the featherseal is indicated in each figure (at $X/P=0$), with a height of $Z/S=0$ representing the endwall.

Figure 10(*a*) shows for the low flow condition near the leading edge of the featherseal, the coolant flow is swept toward the pressure side of the blades, remaining near the platform. The additional coolant on the left side of the featherseal is coolant from the front slot leakage. As the flow out of the featherseal is increased, the thermal field measurements in Fig. 10(*b*) show a higher penetration of the coolant into the passage. These thermal field measurements near the leading edge of the blades indicate that the coolant from the upstream slot is affected when the coolant is increased from the featherseal. Figure 10(*a*) indicates more coolant toward the suction side of the featherseal than does Fig. 10(*b*).

Although the coolant from the front part of the featherseal is swept toward the pressure side of the blades, the coolant from the aft portion of the featherseal is swept toward the suction side of the blades. Figures 11(*a*) and 11(*b*) show the thermal fields measured near the trailing edge of the slot for the 0.25% and 0.75% featherseal flows. Unlike the leading edge measurements, the aft thermal rake measurements show flow that has been entrained in a vortex-like structure. Since the aft featherseal provides cooling to the platform, this cloud of coolant is from the midpassage featherseal flow that is swept off the platform. When the flow out of the featherseal is increased, as show in Fig. 11(*b*), the coolant entrained in the vortex flow is higher off the platform. Increased featherseal flow provides no additional platform cooling.

Comparisons to Computations

A number of computational simulations were conducted to better understand the leakage flow, as indicated in Table 3. Figure 12

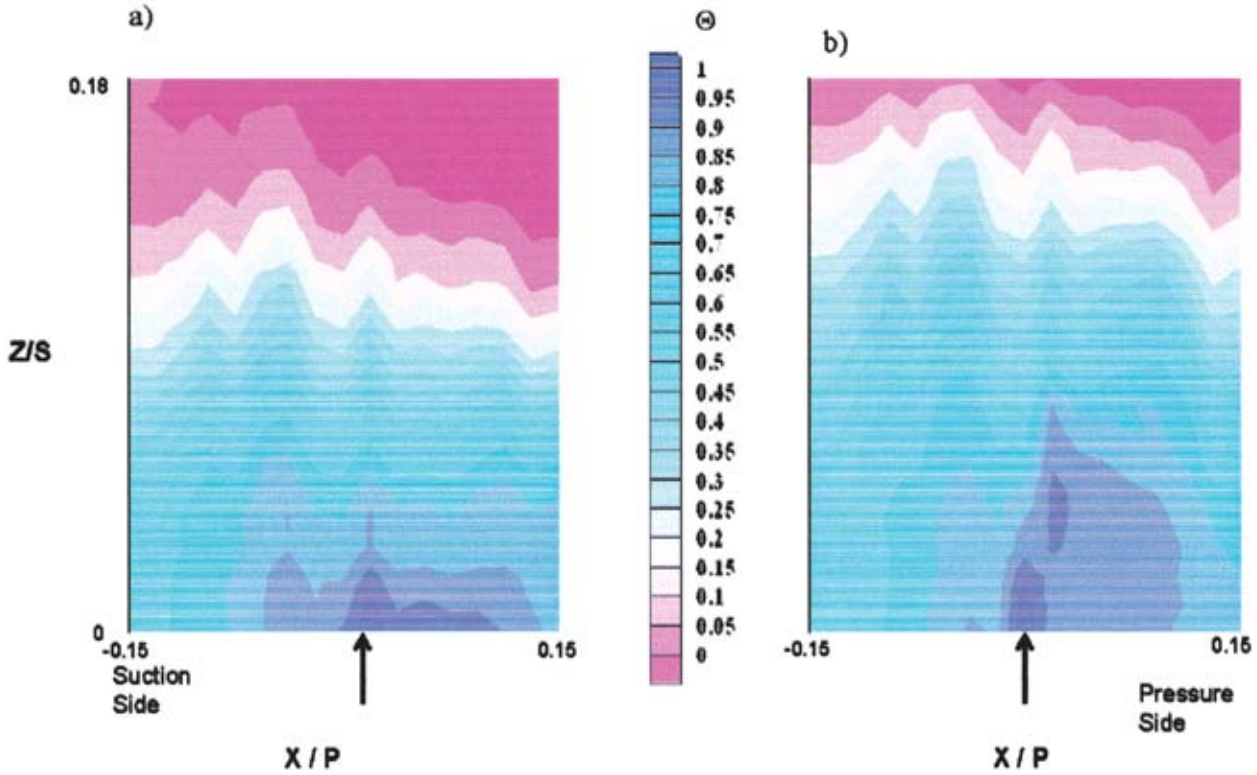

Fig. 10 Thermal rake measurements along the leading edge of the featherseal with 1.5% front slot flow for (*a*) 0.25% featherseal and (*b*) 0.75% featherseal flow

shows the adiabatic effectiveness measurements from the computational simulation with 1.5% upstream and downstream slot flows, and 0.25% featherseal flow. Although the computational predictions match the trends shown in the experimental data, the adiabatic effectiveness levels are overpredicted. We expect the cause of these overpredictions is a function of the near-wall turbulence modeling and a slight mismatch of the experimental inlet pressure conditions.

For both experimental and computational cases, there is little cooling on the pressure side of the blades, especially near the

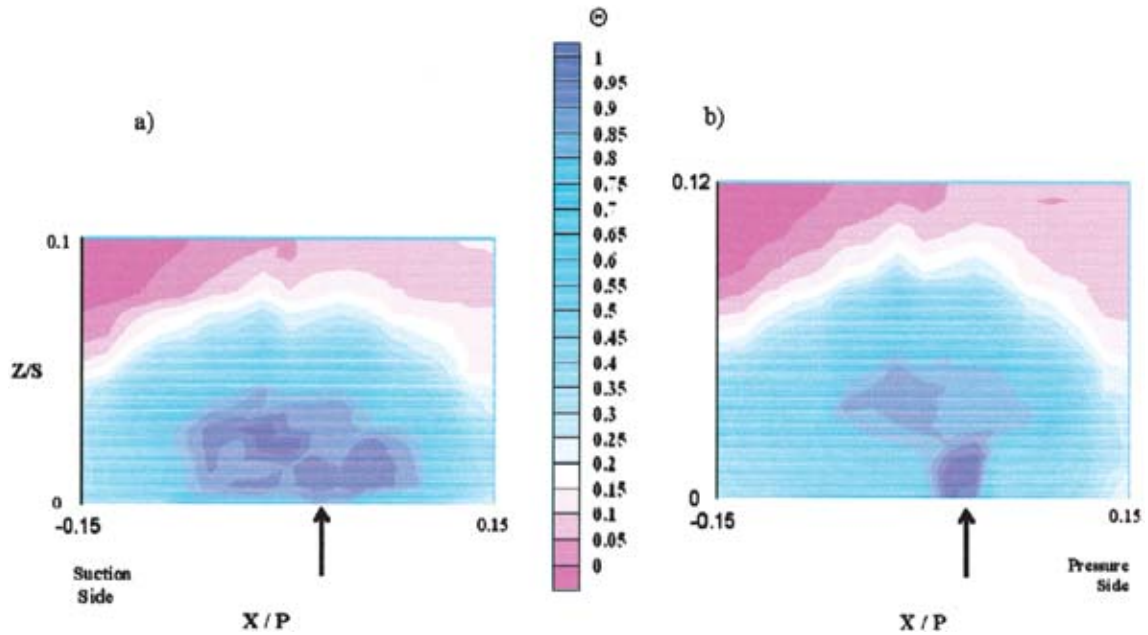

Fig. 11 Thermal rake measurements along the trailing edge of the featherseal with 1.5% front slot flow for (*a*) 0.25% featherseal and (*b*) 0.75% featherseal flow

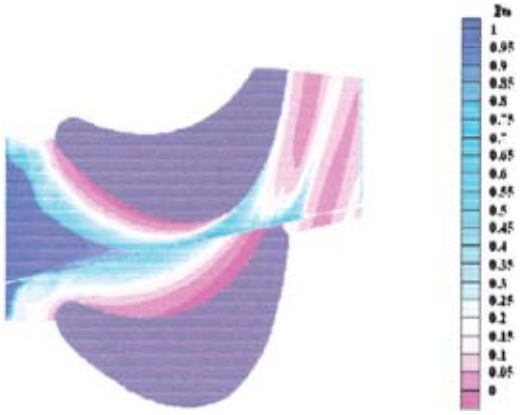

Fig. 12 Computational predictions for 1.5% front and aft slot flow and 0.25% featherseal flow

trailing edge. In both the computational and experimental data, the endwall effectiveness levels along the featherseal appear to decrease toward the trailing edge. The predicted effectiveness values near the suction side of the blades were lower than the experimentally measured values. However, these differences are attributed to the higher predicted values from the front rim.

To observe the leakage flows out of the featherseal, streamlines colored by height were released from the featherseal. Figure 13 shows streamlines released from the featherseal plenum with a flow of 0.25% and an upstream and aft slot flows each at 1.5%. The streamlines show the characteristics of the featherseal flow that were observed in the experimental testing. The streamlines are swept toward the pressure side of the blades near the leading edge followed by a sweeping toward the suction side of the blades near the trailing edge. Additionally, the secondary flows lift the featherseal off the platform in the midpassage. This lifted flow was observed in the trailing edge thermal rake measurements (Figs. 11(*a*) and 11(*b*)). Toward the trailing edge of the featherseal, the streamlines remain on the platform, providing a film cooling layer.

Computational results with higher featherseal and upstream slot flows also matched the trends measured with the experimental cases. While increases in front slot cooling from 1.5% (Fig. 14(*a*)) to 2.0% with 0.25% featherseal flow (Fig. 14(*b*)) increases the cooling of the platform region, increases in featherseal to 0.75% cooling with 2.0% front slot flow (Fig. 14(*c*)) do not provide any additional platform cooling. While front slot cooling is overpredicted, similar trends are observed.

To further compare the computational and experimental results, we calculated averaged adiabatic effectiveness values for both cases, shown in Fig. 15. As expected, near the leading edge the computational values are higher since the front slot cooling was

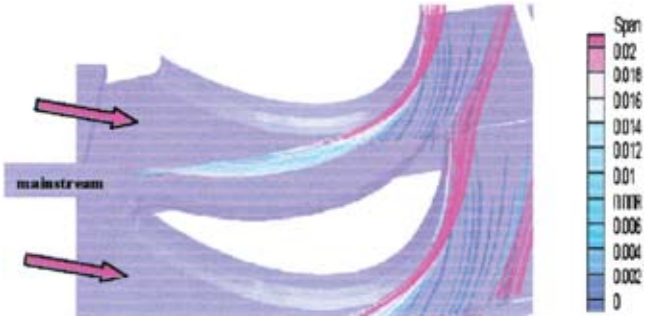

Fig. 13 Computational streamlines colored by height from the featherseal for 0.25% flow, with 1.5% front rim flow (not shown for clarity)

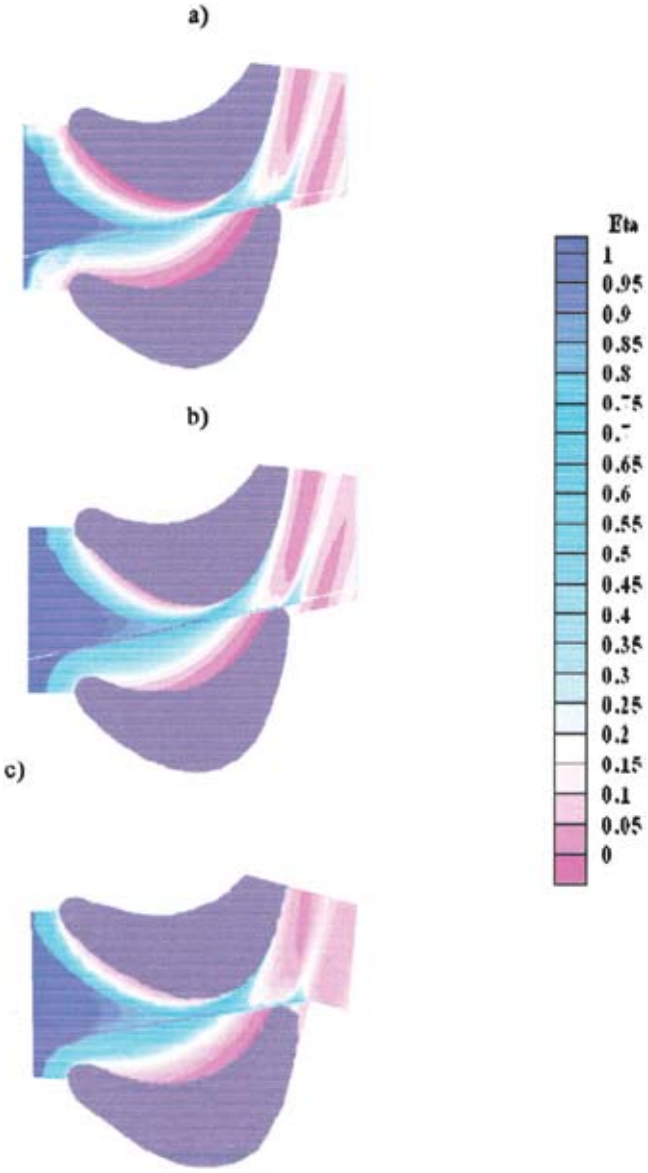

Fig. 14 Computational predictions for (*a*) 1.5% front slot and 0.25% featherseal, (*b*) 2.0% front slot and 0.25% featherseal, and (*c*) 2.0% front slot and 0.75% featherseal, all with 1.5% aft slot flow

overpredicted. However, the trends for both lines show that the computational predictions were able to match the experimental flows in the midpassage. Figure 15 shows a cooling advantage to increasing the front slot flow, while increases from the featherseal (Fig. 7) do not.

To determine if momentum flux changes in the flow from the featherseal caused the different flows out of the featherseal (as shown in Fig. 13), the computational results were used to calculate the momentum flux at the locations of the thermal rake measurements. Based upon the inviscid mainstream velocity at midspan and the static pressure measurements along the platform, a local momentum flux ratio of 1.22 (based on local velocities) was calculated for the leading edge of the featherseal, and a ratio of 1.3 was calculated for the trailing edge featherseal. Given nearly the same momentum flux, the secondary flow field affects must be causing the effects in featherseal coolant. The crossover flow from the featherseal, shown in both computational and experimental measurements, lifts the featherseal flow off the platform. These secondary cooling flows in the midpassage were observed by the

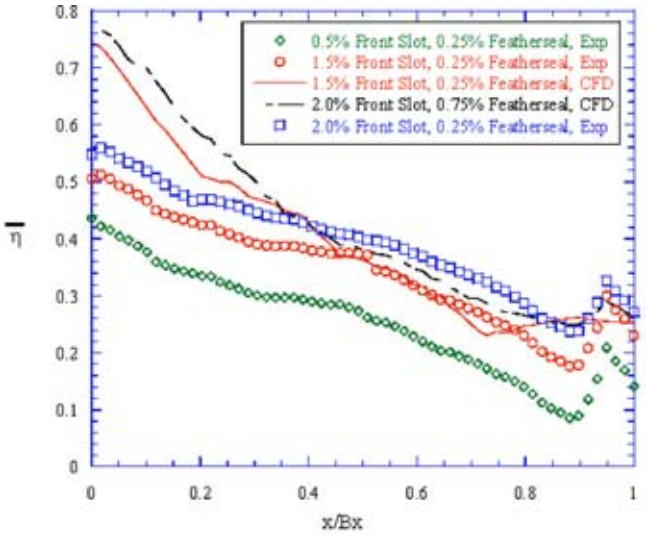

Fig. 15 Average adiabatic effectiveness measurements for the experimental data and computational predictions

thermal rake measurements along the trailing edge of the featherseal. The results in Figs. 11(*a*) and 11(*b*) are not showing the flow from that specific featherseal location being affected by the secondary flows; instead, they show the coolant vortex that is formed upstream of the thermal rake location by the secondary flows and carried down the passage.

Conclusions

Numerous simulations have been performed to address effects of leakage flows on platform cooling. The resulting adiabatic effectiveness distributions along the endwall matched many of the results observed in open literature, showing coolant from a backward-facing upstream slot provides cooling to the endwall. Although coolant was present through 50% of the blade passage, little cooling was provided to either side of the trailing edges of the blades.

Increases of flow from the midpassage featherseal slot provided little additional cooling benefits to the blade platform, with the exception being near the trailing edge of the blades. At the passage inlet, the inlet angle of the mainstream flow swept the featherseal leakage coolant towards the pressure side of the blades. Further into the blade passage, the cross-passage pressure differential between the blades swept the featherseal coolant back toward the suction side of the blades.

Laterally averaged adiabatic effectiveness measurements showed that increases in featherseal leakage did not provide an additional cooling benefit while increases in the upstream slot flow did provide additional cooling benefit to the endwall. This lack of cooling with increased featherseal flow was further quantified with thermal field measurements. The thermal fields indicated the effects of the passage vortex in the blade passage.

While the coolant flow through the trailing edge of the slot was higher than through the leading edge, the local momentum flux ratio across the featherseal remains relatively constant. Additionally, the location of featherseal crossover, which is the location where the coolant direction is changed from being directed toward the suction surface rather than pressure surface, is independent of featherseal and front slot flows.

The results from this study lead us to the conclusion that there should be tighter seals for the featherseal between the adjacent blades to minimize coolant leakage since there is relatively little benefit in terms of endwall cooling. The benefit realized from the upstream leakage, however, is more pronounced for the endwall but still limited to selected regions.

There are several recommendations for future work, based upon the results of these experiments. First, repeating these experiments with a heated, conductive platform would allow for heat transfer coefficients to be calculated for the entire hub region. Additionally, pressure loss measurements in the passage would quantify any negative effects in efficiency caused by leakage flows. By examining the effects of different front slot entrance angles, mismatched featherseal gap heights, and larger coolant leakages, improvements of hub cooling will be made.

Acknowledgments

The authors would like to acknowledge support from Pratt & Whitney for the work presented in this paper. In particular, John Wiedemer and Mike Blair are to be thanked for their contributions. Additionally, Erik Hohlfeld provided some of the initial computational results and mesh adaptions.

Nomenclature

B_x = axial chord
C = true chord
C_p = static pressure coefficient, $(P_{s,\text{local}}-P_{s,\text{inlet}})/P_{\text{dyn}}$
I = momentum flux ratio $(\rho_c V_c^2/\rho_\infty V_\infty^2)$
P = blade pitch
$P_{d,\text{in}}$ = dynamic pressure at the inlet
$P_{s,\text{in}}$ = static pressure at the inlet
$P_{s,\text{local}}$ = local static pressure
Re_C = Reynolds number based on true chord
S = span
s = surface distance along blade from stagnation point
T = temperature
X,Y,Z = wind tunnel coordinate system

Greek

η = adiabatic effectiveness $(T_\infty-T_{\text{aw}})/(T_\infty-T_c)$
θ = nondimensional temperature $(T_\infty-T)/(T_\infty-T_c)$
ρ = density
Δ = denotes a difference

Subscripts and Superscripts

$\bar{}$ = lateral average value
aw = adiabatic wall
av = averaged value
c = coolant conditions
max = maximum value
∞ = mainstream conditions

References

[1] Langston, L. S., Nice, M. L., and Hooper, R. M., 1977, "Three-Dimensional Flow Within a Turbine Cascade Passage," ASME J. Eng. Power, **99**, pp. 21–28.
[2] Graziani, R. A., Blair, M. F., Taylor, J. R., and Mayle, R. E., 1980, "An Experimental Study of Endwall and Airfoil Surface Heat Transfer in a Large Scale Turbine Blade Cascade," Trans. ASME: J. Eng. Gas Turbines Power, **102**, pp. 257–267.
[3] Sharma, O. P., and Buttler, T. C., 1987, "Reynolds Stresses and Dissipation Mechanisms Downstream of a Turbine Cascade," J. Turbomach., **109**, pp. 229–236.
[4] Goldstein, R. J., and Spores, R. A., 1988, "Turbulent Transport on the Endwall in the Region Between Adjacent Turbine Blades," J. Turbomach., **110**, pp. 862–869.
[5] Kang, M. B., Kohli, A., and Thole, K. A., 1999, "Heat Transfer and Flowfield Measurements in the Leading Edge Region of a Stator Vane Endwall," J. Turbomach., **121**, pp. 558–568.
[6] Blair, M. F., 1974, "An Experimental Study of Heat Transfer and Film Cooling on Large-Scale Turbine Endwall," ASME J. Heat Transfer, **96**, pp. 524–529.
[7] Burd, S. W., Satterness, C. J., and Simon, T. W., 2000, "Effects of Slot Bleed Injection Over a Contoured Endwall On Nozzle Guide Vane Cooling Performance: Part II—Thermal Measurements," ASME Paper No. 2000-GT-200.
[8] Colban, W. F., Thole, K. A., and Zess, G., 2003, "Combustor Turbine Interface Studies—Part 1: Endwall Effectiveness Measurements," J. Turbomach., **125**, pp. 203–209.
[9] Zhang, L. J., and Jaiswal, R. S., 2001, "Turbine Nozzle Endwall Film Cooling Study Using Pressure Sensitive Paint," J. Turbomach., **123**, pp. 730–738.

[10] Nicklas, M., 2001, "Film-Cooled Turbine Endwall in a Transonic Flow Field: Part II—Heat Transfer and Film-Cooling Effectiveness," J. Turbomach., **123**, pp. 720–729.
[11] Knost, D. G., and Thole, K. A., 2003, "Computational Predictions of Endwall Film-Cooling for a First Stage Vane," ASME Paper No. GT2003-38252.
[12] Yu, Y., and Chyu, M. K., 1998, "Influence of Gap Leakage Downstream of the Injection Holes on Film Cooling Performance," J. Turbomach., **120**, pp. 541–548.
[13] Aunapu, N. V., Volino, R. J., Flack, K. A., and Stoddard, R. M., 2000, "Secondary Flow Measurements in a Turbine Passage With Endwall Flow Modification," J. Turbomach., **122**, pp. 651–658.
[14] Chung, J. T., and Simon, T. W., 1993, "Effectiveness of the Gas Turbine Endwall Fences in Secondary Flow Control at Elevated Freestream Turbulence Levels," ASME Paper No. 93-GT-51.
[15] The Mathworks Inc., MATLAB, Version 6.5, Release 13, 2002 (Massachusetts).
[16] Fluent Inc., FLUENT User's Guide, Version 6.0, 2002 (New Hampshire).